9. B. Asfaw *et al., Nature* **416**, 317 (2002).
10. J. Hawks *et al., J. Hum. Evol.* **39**, 1 (2000).
11. C. Stringer, *Philos. Trans. R. Soc. London Ser. B* **357**, 563 (2002).
12. R. L. Holloway, in *Handbook of Human Symbolic Evolution*, A. Lock, C. R. Peters, Eds. (Blackwell, Oxford, 1999), pp. 74–125.
13. T. Jacob, in *Homo erectus: Papers in Honor of Davidson Black*, B. A. Sigmon, J. S. Cybulski, Eds. (Univ. of Toronto Press, Toronto, Canada, 1981), pp. 87–104.
14. S. Matsu'ura *et al., Curr. Anthropol.* **41**, 297 (2000).
15. E. Delson *et al., Anat. Rec.* **262**, 380 (2001).
16. Vertebrate fossils recovered from the Sm 4 findspot vary in preservation, suggesting a mixed assemblage composed of fossils from multiple sources upstream. Outcrops that we identified, within 6 km upstream of the find, include those that belong to the traditional Kabuh Formation of this area. On the basis of its adhering matrix, Sm 4 is likely to have derived from this series.
17. F. Weidenreich, *Anthropol. Pap. Am. Mus. Nat. Hist.* **43**, 205 (1951).
18. F. Weidenreich, *Palaeontol. Sin. New Ser. D* **10**, 1 (1943).
19. Materials and methods are available as supporting material on *Science* Online.
20. H. Seidler *et al., J. Hum. Evol.* **33**, 691 (1997).
21. Our micro-CT analysis of Ngandong 12 revealed a damaged clivus and missing dorsum sellae, tuberculum sellae, and planum sphenoideum regions. This precludes a numerical evaluation of its cranial base flexion. The entire region from the sella turcica to the planum sphenoideum is missing in Sangiran 17. However, the floor of the sella turcica is preserved in Ngandong 12, and the clivus in Sangiran 17, allowing a comparison of approximate alignments with Sm 4 (Fig. 2, G and H). This suggests a cranial base, in both Ngandong 12 and Sangiran 17, that is broadly compatible with the Sm 4 condition of flexion. As far as we are aware, no account of cranial base flexion of Ngandong 7 has been published.
22. C. Ross, M. Henneberg, *Am. J. Phys. Anthropol.* **98**, 575 (1995).
23. F. Spoor, *Am. J. Phys. Anthropol. Suppl.* **30**, 288 (2000).
24. D. E. Lieberman, C. F. Ross, M. J. Ravosa, *Yrbk. Phys. Anthropol.* **43**, 117 (2000).
25. D. E. Lieberman, B. M. McBratney, G. Krovitz, *Proc. Natl. Acad. Sci. U.S.A.* **99**, 1134 (2002).
26. In Sm 4, the anterior temporal pole outline intersects the midline cranial base profile close to the tuberculum sellae, whereas the same intersection in modern humans occurs at a position approximately at the middle of the planum sphenoideum (Fig. 2, I and J).
27. F. Spoor, P. O'Higgins, C. Dean, D. E. Lieberman, *Nature* **397**, 572 (1999).
28. M. Bhat, D. E. Enlow, *Angle Orthodont.* **55**, 269 (1985).
29. F. Bookstein *et al., Anat. Rec.* **257**, 217 (1999).
30. S. Antón, S. Marquez, K. Mowbray, *J. Hum. Evol.* **43**, 555 (2002).
31. G. Hewitt, *Nature* **405**, 907 (2000).
32. G. D. van den Bergh, J. de Vos, P. Y. Sondaar, *Palaeogeogr. Palaeoclimatol. Palaeoecol.* **171**, 385 (2001).
33. F. J. Gathorne-Hardy, Syaukani, R. G. Davies, P. Eggleton, D. T. Jones, *Biol. J. Linn. Soc.* **75**, 453 (2002).
34. R. C. McCarthy, *J. Hum. Evol.* **40**, 41 (2001).
35. F. Spoor, *S. Afr. J. Sci.* **93**, 182 (1997).

36. We thank Darsono for the recovery of Sm 4; Sudijono, T. Sihombing, I. Kurniawan, A. Hikmat, E. Indriati, A. Suprijo, P. H. Sulistyarto, R. A. Suriyanto, J. M. Susanto, and people of Mlale and Cemeng for fieldwork; J. Arif for access to Tjg-1993.05; H. Otsuka for stratigraphic interpretations; T. Suzuki for observations of possible traumatic bone alteration on Sm 4; F. Spoor for comments on *H. erectus* cranial base lengths and flexion; S. Matsukawa and M. Chubachi for assistance; and T. White and E. Delson for suggestions. We thank the Geological Research and Development Centre, Bandung, for permission and support. This work was supported by the National Science Museum, Tokyo, and the Japan Society for the Promotion of Science.

Supporting Online Material
www.sciencemag.org/cgi/content/full/299/5611/1384/DC1
Materials and Methods
Fig. S1
Tables S1 and S2

19 December 2002; accepted 27 January 2003

Foraging Adaptation and the Relationship Between Food-Web Complexity and Stability

Michio Kondoh

Ecological theory suggests that complex food webs should not persist because of their inherent instability. "Real" ecosystems often support a large number of interacting species. A mathematical model shows that fluctuating short-term selection on trophic links, arising from a consumer's adaptive food choice, is a key to the long-term stability of complex communities. Without adaptive foragers, food-web complexity destabilizes community composition; whereas in their presence, complexity may enhance community persistence through facilitation of dynamical food-web reconstruction that buffers environmental fluctuations. The model predicts a linkage pattern consistent with field observations.

Ecological theory (*1*–*5*) suggests that complexity (high species richness, dense trophic links) destabilizes food webs. "Real" ecosystems often support large numbers of species interacting in highly complex networks of direct and indirect pathways (*6*–*9*). To resolve this apparent paradox, several hypotheses have been proposed, including ones attributing "real" food-web stability to dominance of stabilizing food-web architecture (*10*, *11*). These studies have considered relatively static topological food-web features such as distribution of interaction strength (*10*) and trophic links (*11*). I propose that "flexibility" in food-web structure, arising from the consumers' adaptive behavioral (*12*, *13*) or evolutionary (*14*, *15*) switches in food choice in response to qualitative and quantitative resource changes, stabilizes complex food webs.

Adaptation is critical to food-web dynamics (*16*) and influences food-web stability (*17*). This study considers food-web models having more realistic and wide-ranging complexity, where the degree of flexibility is manipulated by systematically changing both the fraction of adaptive foragers and their adaptation rate. This provides a comprehensive picture of the synergistic effects of food-web complexity and adaptation on food-web stability.

Consider a food web comprising N species, any pair of which are connected to each other with probability C (≤ 1; connectance). In determining trophic link direction, I used two models, random (*18*) and cascade (*4*, *18*), which generate different substructures (*19*). Suppose that consumers cannot consume different resource species simultaneously because of the prey's patchy distribution (*12*), the capturing strategy for different prey (*12*), or the consumer's sensory and cognitive constraints for discriminating between prey (*20*). Consumers allocate their foraging effort among possible resources and, given a fixed total foraging effort (measured by energy or time), per capita consumption rate would increase with increasing foraging efficiency and increased foraging effort allocated to the resource (*21*).

The dynamics of species i ($1 \ldots N$) biomass, X_i, is described by:

$$\frac{dX_i}{dt} = X_i\left(r_i - s_iX_i + \sum_{j \in resources} e_{ij}f_{ij}a_{ij}X_j - \sum_{j \in consumers} f_{ji}a_{ji}X_j\right) \qquad (1)$$

where r_i is an intrinsic reproductive rate; s_i a self-regulation intensity; f_{ij} the foraging efficiency of species i on resource species j, defined as a per capita foraging rate when all foraging efforts are allocated to resource j; a_{ij} the foraging effort of species i allocated to resource j ($\sum_{j \in resources} a_{ij} = const. = 1$, and $a_{ij} = 0$ when species i does not feed on species j); and e_{ij} the metabolic rate of species i consuming species j. Hereafter, e_{ij} is, for simplicity, set to a biologically feasible (*22*, *23*) constant value, e (here $e = 0.15$, but for $e = 0.01$ to 0.35 the value does not alter the main result).

I used community persistence, the probability that all species persist for a given time in fluctuating environments, as an index of food-web stability. As biological parameters change over space and time by environmental disturbances, the community persisting in the wider parameter region is more likely to be observed in nature (*3*). To estimate the effects of complexity on community persistence, I calculated the probability of community persistence in an ensemble of stochastically gen-

---

Center for Ecological Research, Kyoto University, Kamitanakami, Otsu 520-2113, Japan.

Present address: Cardiff School of Biosciences, Cardiff University, Post Office Box 915, Cardiff CF10 3TL, UK. E-mail: kondohm@cf.ac.uk

erated food-web models with varying complexity (N, C) (*24*). When species population density becomes very low ($X_i < 10^{-13}$), the species is permanently removed, which represents extinction.

Consider an extreme case where a food web contains no adaptive foragers. As no individual species discriminate between resources, foraging efforts are equally allocated among all possible resource species [a_{ij} = 1/(*the potential number of species* i*'s resource species*)]. Irrespective of the food-web model, persistence decreases with increasing species richness or connectance (Fig. 1, A, B, and G), agreeing with previous models (*1*–*5*) that use different stability indices and/or food-web structures. The negative effect of species richness on stability is detectable even if persistence is measured by a species' extinction probability [ln(*persistence probability*)/N], and results in rejection of the null hypothesis that ascribes this negative relationship to an increased number of species with the same extinction probability.

In reality, trophic link strength is not a fixed property. Consumers switch foraging behavior at individual levels (*12*, *13*, *25*, *26*) and foraging-related traits may evolve at population levels (*14*, *27*). In the presence of adaptive foragers, the observed connection probability {"realized connectance"; (*total number of links*)2/[N(N–1)]} can be smaller than C (renamed "potential connectance"), as some potential resources may not be used. The dynamics of the foraging effort of an adaptive consumer i to resource species j (a_{ij}) is given by (*21*):

$$\frac{da_{ij}}{dt} = G_i a_{ij}\left(e_{ij} f_{ij} X_j - \sum_{k \in resources} a_{ik} e_{ik} f_{ik} X_k\right) \qquad (2)$$

where j is the potential prey of species i; G_i the adaptation rate of consumer i, which is higher when species change their diet behaviorally rather than evolutionarily, when the evolutionary speed is higher, or when the species that shifts its diet behaviorally has more detailed and complete information about resources or better information-processing ability (*12*). Eq. 2 represents a simple food-choice rule that maximizes energy gain (*21*): a consumer species i increases its foraging effort allocated to resource j if resource profitability, energy gain per unit effort ($e_{ij} f_{ij} X_j$), is higher than the average profitability of resources that the consumer is currently foraging ($\sum_{k \in resources} a_{ik} e_{ik} f_{ik} X_k$ as $\sum_{k \in resources} a_{ik} = 1$).

It will decrease its effort if profitability is lower than average. A consumer will only feed on the most profitable prey if adaptation is extremely rapid; slow adaptation leads to time delay in food choice and, in a fluctuating environment, may cause asynchrony between food choice and food profitability.

To investigate how adaptive food choice alters the complexity-stability relationship, consider a fraction, F, of randomly chosen species shifting their diet ($G_i > 0$), while the remaining fraction (1 – F) cannot ($G_i = 0$); for simplicity, adaptation rates are set to a constant (G). The population dynamics of such a food web is governed by combining population dynamics (Eq. 1) and adaptive dynamics (Eq. 2). With adaptive foragers, there is a critical level of complexity [the line along the diagonal ridge of parameter space of species richness and connectance (Fig. 1E)], where stability is prohibited below and promoted above by increasing complexity. With decreasing fraction of adaptive foragers, F (Fig. 1, E to G), or adaptation rate, G (Fig. 1, E, H, and I), the region of positive relationship decreases and the relationship becomes less clear. Regardless of model used, these outcomes were not altered qualitatively, which suggests that the robustness of the basic premise that increasing the fraction of adaptive foragers or their adaptive ability can turn negative complexity-stability relationships into positive ones.

The model predicts that realized connectance should depend on the observation time scale (*28*, *29*). Suppose biological parameters change intermittently with sufficiently long intervals. Within a short time range, the realized connectance may be represented by a single parameter set. At this scale, complex food webs

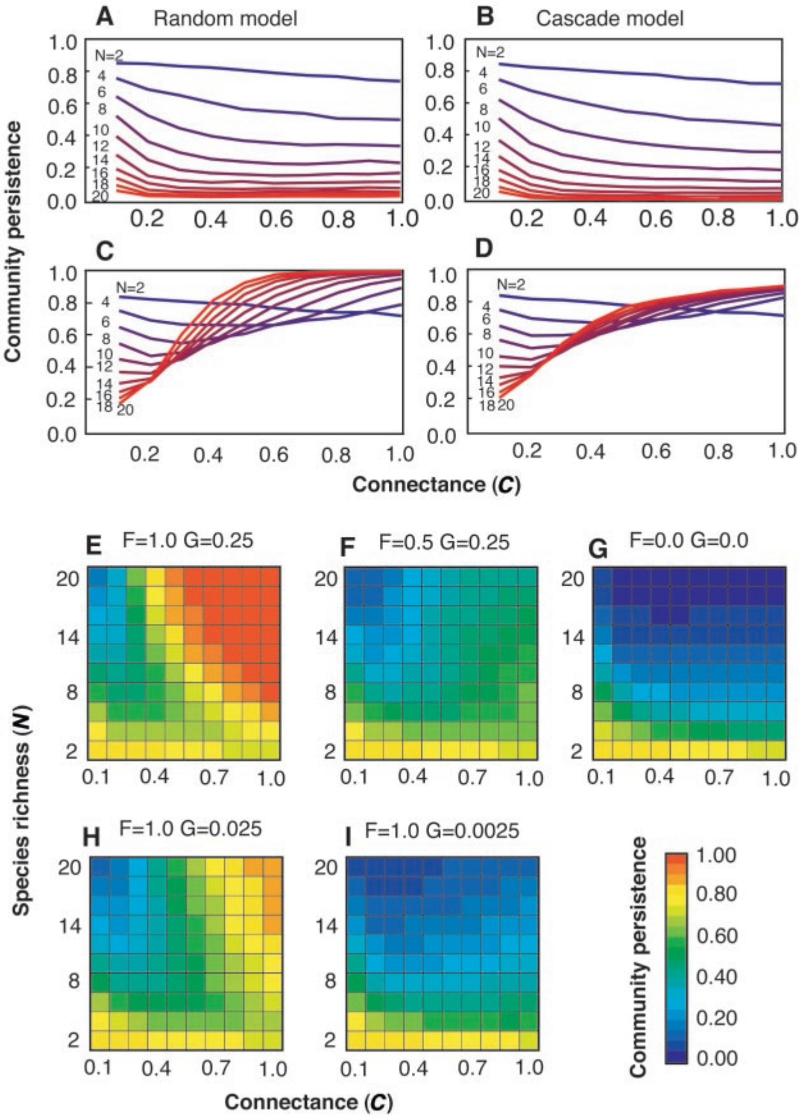

Fig. 1. Relationships between food-web complexity and stability. (**A** to **D**) Complexity-stability relationship in food webs without (A, B) or with (C, D) adaptive foragers in random (A, C) and cascade (B, D) models. (**E** to **I**) Complexity-stability relationships with varying (E to G) fraction of adaptive foragers (F) or (E, H, and I) adaptation rate (G) in the random model. Parameters are (F, G) = (A, B) (0.0, 0.0), (C, D) (1.0, 0.25).

with adaptive foragers are characterized by a few strong (high foraging effort, a_{ij}) and many weak (low foraging effort) links (Fig. 2A). This is a consistent pattern recorded from observations (*6*, *30*–*32*) of natural food webs. The realized connectance becomes upper-bounded (Fig. 2B) with increasing potential connectance (C), and its maximum level decreases with increasing fraction of adaptive forgers (F) (Fig. 2B). This pattern implies that adaptive foragers use only a part of their potential resources. At a longer time scale, environmental disturbances lead to fluctuating selection on interaction strength and consequently food-web reconstruction (Fig. 3, supporting online text). The realized connectance should increase with observation time as the probability of a potential link's activation increases and will approach potential connectance (C) when the observation period is infinitely long. This time scale–dependent linkage pattern indicates that high complexity affords food webs high "flexibility"; potential links are activated or inactivated while realized connectance is kept low in response to environmental changes and population fluctuations to enhance community persistence.

This mechanism demands sufficiently high adaptation speed to induce quick food-web reconstruction when disturbance takes place. Empirical evidence of fast evolution of foraging-related traits (*14*, *15*, *27*, *33*) indicates that evolution and population dynamics may overlap temporally. Changes in adaptive learning associated with foraging behavior is not restricted to higher animals but is frequently observed in arthropods (*25*, *26*), this suggests that behavioral diet shifts, which occur over shorter time scales than a generation, may be widespread to those taxa. Adaptive diet choice may potentially have a major influence on community dynamics. Precise empirical studies are required to test explicitly whether the dynamic changes in food-web linkage observed in nature (*6*, *28*, *29*, *34*) are attributed to adaptation.

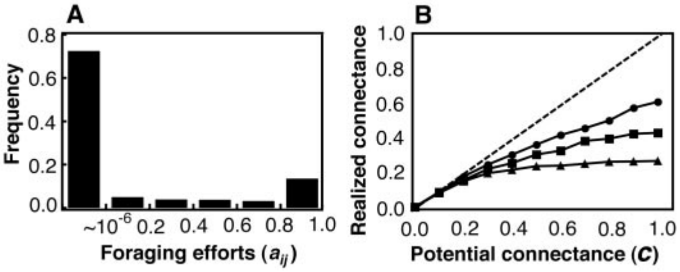

Fig. 2. Short-term linkage patterns of food webs. (**A**) Frequency distribution of realized foraging efforts (a_{ij}; in 1000 persistent communities) in food webs with adaptive foragers ($F = 1.0$). Parameters: $N = 12$, $C = 1.0$, $G = 0.25$, $t = 10^5$. (**B**) The effect of potential connectance (C) on the realized connectance (fraction of links with $a_{ij} > 10^{-6}$ averaged over 100 simulations) of food web with low (circle; $F = 0.5$), intermediate (square; 0.75), and high (triangle; 1.0) proportion of adaptive foragers. Without adaptive foragers ($F = 0.0$), realized connectance ≡ potential connectance (dotted line). Parameters: $N = 12$, $C = 1.0$, $G = 2.5$, $t = 10^5$.

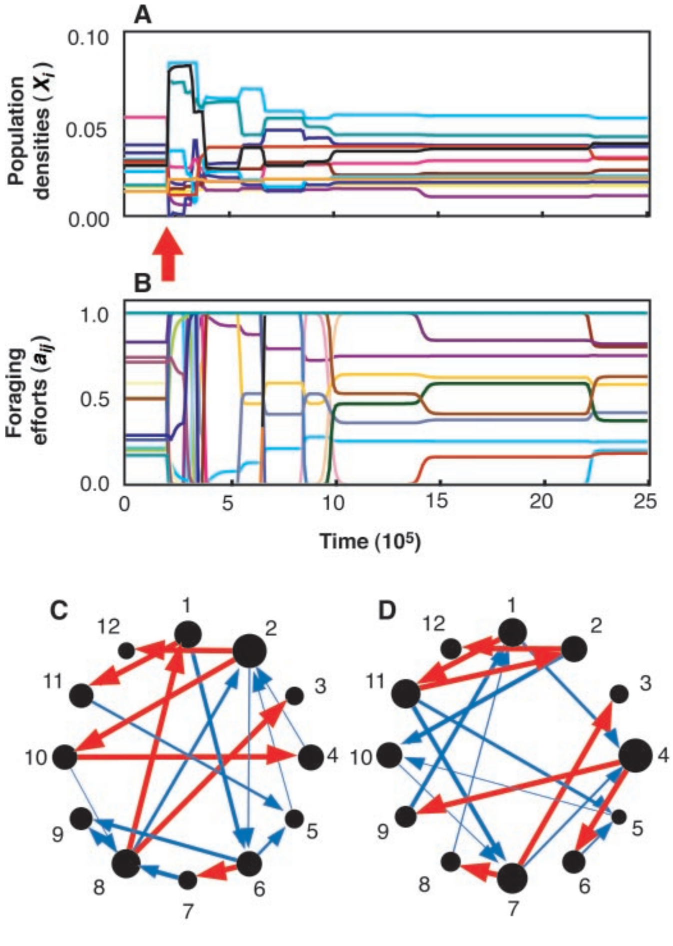

Fig. 3. An example of long-term food-web dynamics. A random model with parameters $N = 12$, $C = 1.0$, $F = 1.0$, $G = 0.025$. Disturbance (indicated by red arrow at $t = 2 \times 10^5$), which randomly changes parameters, r_i and f_i, leads to (**A**) population fluctuation accompanied by (**B**) dynamical changes in foraging efforts. Different colors represent (A) 12 species and (B) 66 trophic links between them. (**C** and **D**) Food-web architecture and interaction strength before (C, $t = 2 \times 10^5$) and after (D, $t = 2 \times 10^6$) the disturbance. Red and blue arrows are trophic links with foraging effort (a_{ij}) of larger and smaller than 0.9, respectively. Thickness of arrows and circle sizes represent foraging efforts (a_{ij}) and species densities (X_i), respectively. Links with foraging efforts smaller than 0.1 are not depicted.

This study has implications for conservation. Biodiversity loss effects on community stability will be influenced by the focal community's evolutionary history, as complexity-stability relationships depend on the developmental levels of foraging-adjustment ability that are shaped through natural selection (*13*). Introduced species, which do not share an evolutionary history with local organisms, can influence community stability in a manner different from that of resident species or populations. A positive relationship between species richness and community stability suggests that high biodiversity is self-sustaining. In such cases, losses of species may catalyze further losses for system instability and the effort required to prevent the next loss would increase as the number of loss increases. If present species diversity levels are maintained through natural selection on foraging behavior, the genetic structure of populations may influence community level dynamics through change in adaptation rate. This implies an important link between the genetic and community levels of biology.

References and Notes

1. R. M. May, *Nature* **238**, 413 (1972).
2. S. L. Pimm, J. H. Lawton, *Nature* **268**, 329 (1977).
3. S. L. Pimm, *The Balance of Nature?* (Univ. of Chicago Press, Chicago, 1991).
4. X. Chen, J. E Cohen, *J. Theor. Biol.* **212**, 223 (2001).
5. X. Chen, J. E. Cohen, *Proc. R. Soc. London Ser. B* **268**, 869 (2001).
6. K. O. Winemiller, *Ecol. Monogr.* **60**, 331 (1990).
7. N. D. Martinez, *Ecol. Monogr.* **61**, 367 (1991).
8. G. A. Polis, *Am. Nat.* **138**, 123 (1991).
9. L. Goldwasser, J. Roughgarden, *Ecology* **74**, 1216 (1993).
10. R. V. Solé, J. M. Montoya, *Proc. R. Soc. London Ser. B* **268**, 2039 (2001).
11. A.-M. Neutel, J. A. P. Heesterbeek, P. C. de Ruiter, *Science* **296**, 1120 (2002).
12. D. W. Stephens, J. R. Krebs, *Foraging Theory* (Princeton Univ. Press, Princeton, 1987).
13. A. A. Agrawal, *Science* **294**, 321 (2001).
14. A. Joshi, J. N. Thompson, *Evolution* **51**, 846 (1997).
15. J. N. Thompson, *Trends Ecol. Evol.* **13**, 329 (1998).
16. P. A. Abrams, in *Food Webs: Integration of Pattern and Dynamics*, G. A. Polis, K. O. Winemiller, Eds. (Kluwer Academic Publishers, Norwell, MA, 1996), pp. 113–121.
17. P. A. Abrams, *Annu. Rev. Ecol. Syst.* **31**, 79 (2000).
18. J. E., Cohen, F. Briand, C. M. Newman, *Community Food Webs: Data and Theory* (Springer-Verlag, Berlin, 1990).
19. In a random model, consumer and resource roles are assigned at random to two interacting species. The model has a maximal degree of freedom and generates food webs with complex substructure consid-

ered common in real food webs (*6*–*9*). The cascade model assumes a hierarchical relationship between species that constrains the trophic role as consumer or resource: hierarchically higher species are always feeding on species with a lower ranking. This model cannot generate any loops, but explains some important properties of natural food webs such as the species richness among trophic levels (*18*).

20. E. A. Bernays, D. J. Funk, *Proc. R. Soc. London Ser. B* **266**, 151 (1999).
21. H. Matsuda, M. Hori, P. A. Abrams, *Evol. Ecol.* **10**, 13 (1996).
22. W. F. Humphreys, *J. Anim. Ecol.* **48**, 427 (1979).
23. C. T. Robbins, *Wildlife Feeding and Nutrition* (Academic Press, London, 1983).
24. I iterated simulation runs with randomly chosen parameter sets ($r_i = 0.0$ to 0.1, $f_{ij} = 0.0$ to 1.0, $s_i = 1.0$), initial abundances ($X_i = 0.0$ to 0.1) and linkage patterns, and measured the frequency of all species co-occurring ($X_i > 10^{-13}$ for all i) after sufficiently long periods ($t = 10^5$ by which time community persistence reaches an asymptote) in 10^4 runs. As in other models (*1*, *3*–*5*), every species persists (with positive equilibrium biomass, r_i / s_i) in the absence of interspecific interaction (food web being always persistent when $C = 0$), they are either autotrophs or use external resources (*35*). This assumption avoids a confounding effect (*36*) of an increase in interspecific links decreasing the number of heterotrophic species with no potential diet present in the web.
25. R. Dukas, E. A. Bernays, *Proc. Natl. Acad. Sci. U.S.A.* **97**, 2637 (2000).
26. M. Egas, M. W. Sabelis, *Ecol. Lett.* **4**, 190 (2001).
27. M. Hori, *Science* **260**, 216 (1993).
28. G. P. Closs, P. S. Lake, *Ecol. Monogr.* **64**, 1 (1994).
29. A. F. Tavares-Cromar, D. D. Williams, *Ecol. Monogr.* **66**, 91 (1996).
30. R. T. Paine, *Nature* **355**, 73 (1992).
31. D. G. Raffaelli, S. J. Hall, in *Food Webs: Integration of Pattern and Dynamics*, G. A. Polis, K. O. Winemiller, Eds. (Kluwer Academic, Norwell, MA, 1996), pp. 185–191.
32. J. T. Wooton, *Ecol. Monogr.* **67**, 45 (1997).
33. N. G. Hairston Jr. *et al. Nature* **401**, 446 (1999).
34. K. Schoenly, J. E. Cohen, *Ecol. Monogr.* **61**, 267 (1991).
35. G. A. Polis, S. D. Hurd, in *Food Webs: Integration of Pattern and Dynamics*, G. A. Polis, K. O. Winemiller, Eds. (Kluwer Academic, Norwell, MA, 1996), pp. 275–285.
36. D. L. DeAngelis, *Ecology* **56**, 238 (1975).

37. I thank H. Jones, N. Yamamura, and G. Takimoto for comments. Study partly supported by Japan Society for the Promotion of Science Research Fellowship for Young Scientists.

Supporting Online Material
www.sciencemag.org/cgi/content/full/299/5611/1388/DC1
SOM Text
Figs. S1 and S2
Reference
Movie S1

7 October 2002; accepted 23 January 2003

Phylogenetic Shadowing of Primate Sequences to Find Functional Regions of the Human Genome

Dario Boffelli,[1,2] Jon McAuliffe,[3] Dmitriy Ovcharenko,[2]
Keith D. Lewis,[2] Ivan Ovcharenko,[1,2] Lior Pachter,[4]
Edward M. Rubin[1,2]*

Nonhuman primates represent the most relevant model organisms to understand the biology of *Homo sapiens*. The recent divergence and associated overall sequence conservation between individual members of this taxon have nonetheless largely precluded the use of primates in comparative sequence studies. We used sequence comparisons of an extensive set of Old World and New World monkeys and hominoids to identify functional regions in the human genome. Analysis of these data enabled the discovery of primate-specific gene regulatory elements and the demarcation of the exons of multiple genes. Much of the information content of the comprehensive primate sequence comparisons could be captured with a small subset of phylogenetically close primates. These results demonstrate the utility of intraprimate sequence comparisons to discover common mammalian as well as primate-specific functional elements in the human genome, which are unattainable through the evaluation of more evolutionarily distant species.

Genomic sequence comparisons between distant species have been extensively used to identify genes and determine their intron-exon boundaries, as well as to identify regulatory elements present in the large noncoding fraction of the genome (*1*–*3*). This strategy has been successful in human-mouse comparisons, because the ~75 million years (My) of separation from their last common ancestor have provided sufficient time for a large fraction of nucleotides to have been exposed to considerable mutation and selection pressure. Although such comparisons readily identify regions of the human genome performing general biological functions shared with evolutionarily distant mammals, they will invariably miss recent changes in DNA sequence that account for uniquely primate biological traits.

As a consequence of their short evolutionary separation (apes 6 to 14 My, Old World monkeys 25 My, New World monkeys 40 My) (*4*), there is a paucity of sequence variation between humans and each of their nearest primate relatives. This lack makes it difficult to distinguish functional from passive conservation on the basis of pairwise comparisons, thus limiting the usefulness of such comparisons. However, the additive collective divergence of higher primates as a group (fig. S1) is comparable to that of humans and mice. This suggests that deep sequence comparisons of numerous primate species should be sufficient to identify important regions of conservation that encode functional elements. Phylogenetic footprinting (*5*, *6*) has been used to identify highly conserved putative regulatory elements, exploiting alignments across numerous evolutionarily distant species. We developed a variant of phylogenetic footprinting, which we termed phylogenetic shadowing. In contrast to footprinting, phylogenetic shadowing examines sequences of closely related species and takes into account the phylogenetic relationship of the set of species analyzed. This approach enabled the localization of regions of collective variation and complementary regions of conservation, facilitating the identification of coding as well as noncoding functional regions.

We first examined the ability of this strategy to identify functional regions with precise locations within the human genome, such as intron-exon boundaries. The lack of clone-based libraries for multiple primate species limited us to sequencing orthologous regions from a large set of primates, using genomic DNA as template (*7*). The sole criterion used in the selection of the four different regions that we studied was that each should contain at least one annotated exon. The sequences were generated (*8*) for a set of 13 to 17 primate species that included those evolutionarily closest to humans, such as Old World and New World monkeys and hominoids, but not distant primates such as prosimians. The resulting sequences were analyzed to determine the likelihood ratio under a fast- versus slow-mutation regime for each aligned nucleotide site across all four regions analyzed (supporting online text) (*8*). This ratio represents the relative likelihood that any given nucleotide site was subjected to a faster or slower rate of accumulation of variation and is related to functional constraints imposed on each site. The corresponding likelihood ratio curves were used to describe the variation profile of the four genomic intervals analyzed.

In all regions examined, the exon-containing sequences displayed the least amount of cross-species variation, in agreement with the constraint imposed by their functional role (Fig. 1, A to D). A limited number of short regions of minimal variation similar to the exon-containing sequences appeared in the likelihood plots.

---

[1]U.S. Department of Energy Joint Genome Institute, Walnut Creek, CA 94598, USA. [2]Department of Genome Sciences, Lawrence Berkeley National Laboratory, Berkeley, CA 94720, USA. [3]Department of Statistics, [4]Department of Mathematics, University of California, Berkeley, CA 94720, USA.

*To whom correspondence should be addressed. E-mail: emrubin@lbl.gov